NIH Public Access
Author Manuscript
J Urol. Author manuscript; available in PMC 2010 October 1.

Published in final edited form as:
J Urol. 2009 October ; 182(4): 1600–1607. doi:10.1016/j.juro.2009.06.007.

Electrical Properties of Prostatic Tissues: I. Single Frequency Admittivity Properties

Ryan J. Halter[*], **Alan Schned**, **John Heaney**, **Alex Hartov**, and **Keith D. Paulsen**
Thayer School of Engineering, Dartmouth College (RJH, AH, KDP) and Dartmouth Medical School (AS, JH), Hanover and Dartmouth-Hitchcock Medical Center (AS, JH) and Norris-Cotton Cancer Center (AH, AS, JH, KDP), Lebanon, New Hampshire

Abstract

Purpose—Electrical properties of the prostate may provide sufficient contrast for distinguishing malignant and benign formations in the gland. We evaluated how well these electrical properties discriminate cancer from noncancer tissues in the prostate.

Materials and Methods—Electrical admittivity (conductivity and permittivity) was recorded at 31 discrete frequencies of 0.1 to 100 kHz from each of 50 ex vivo human prostates. A specifically designed admittivity probe was used to gauge these electrical properties from sectioned prostate specimens. The specific tissue area probed was marked to provide precise colocalization between tissue histological assessment and recorded admittivity spectra.

Results—Adenocarcinoma, benign prostatic hyperplasia, nonhyperplastic glandular tissue and stromal tissue were the primary tissue types probed. Mean cancer conductivity was significantly less than that of glandular and stromal tissues at all frequencies ($p < 0.05$), while mean cancer permittivity was significantly greater than that of all benign tissues at 100 kHz ($p < 0.0001$). ROC curves showed that permittivity at 100 kHz was optimal for discriminating cancer from all benign tissues. This parameter had 77% specificity at 70% sensitivity and an ROC AUC of 0.798.

Conclusions—The contrast in electrical admittivity properties of different prostate tissues shows promise for distinguishing cancer from benign tissues. Sensitivity and specificity exceed those reported for current prostate specific antigen screening practices at low prostate specific antigen, making this an attractive addition to the clinical armamentarium for identifying prostate cancer.

Keywords

prostate; prostatic neoplasms; prostatic hyperplasia; electric impedance; spectrum analysis

Prostate cancer is the second leading cause of cancer related death in American males with approximately 28,660 expected to die of the disease in 2008.1 As a result, measuring serum PSA in men older than 50 years was suggested by the American Urological Association and the American Cancer Society as the best means to screen for the disease.2 Despite the success of PSA monitoring to detect earlier stage ACa in the last 2 decades this test leads to a significant number of false-positive findings because PSA is produced by malignant and benign processes.3›4 Alternative PSA based biomarkers, including PSA velocity, free-to-bound PSA ratio, age adjusted PSA, pro-PSA and PSA density, are being investigated in terms of sensitivity and specificity to a significant cancer presence but no concise clinical

[*] Correspondence: Thayer School of Engineering, Dartmouth College, Hanover, New Hampshire 03755 (telephone: 603-646-0773; FAX: 603-646-3856; ryan.halter@dartmouth.edu).

Study received institutional review board approval.

NIH-PA Author Manuscript
NIH-PA Author Manuscript
NIH-PA Author Manuscript

NIH-PA Author Manuscript

NIH-PA Author Manuscript

NIH-PA Author Manuscript

standard has been adopted.5 More specific diagnostic tools that identify ACa requiring therapeutic intervention would decrease the financial burden and help decrease patient anxiety associated with a potential cancer diagnosis.

Electrical properties of the prostate may serve this purpose by providing sufficient contrast for distinguishing between malignant and benign formations in the prostate.6–8 This contrast stems from the biophysical relationship between tissue architecture and its influence on tissue electrical properties. The vastly different cellular and glandular configurations of malignant and benign prostatic tissue provide a spectrum of electrical charge carrying and charge storage capabilities. The term admittivity, which refers to these electrical properties, consists of a conductivity component associated primarily with charge transport (electric current) and a permittivity component associated with charge storage. In tissue the term conductivity defines how easily electric current passes through the medium and permittivity defines how rapidly electric charges accumulate at membranous boundaries. Novel devices are being developed to gauge these properties throughout the prostate9,10 but to our knowledge the potential discriminatory power has not yet been established.

We observed significant differences between the electrical admittivity of cancer and benign tissues in the prostate in a few small pilot studies.7,11 We present our most recent analysis of a larger 50 patient cohort in which we specifically evaluated how well these electrical properties discriminate cancer from noncancer tissues in the prostate.

Materials and Methods

Data Acquisition and Study Group

Electrical properties were gauged across a tissue sample using a 4-electrode (tetrapolar) configuration. The measurement device consists of a parallel set of gold plated ring electrodes deposited on a pair of PCBs (fig. 1). The bottom electrode set is fixed to the probe base and the upper electrode pair translates vertically to allow sample placement. The probe is interfaced through a set of 4 shielded cables to a computer controlled, HP4284A impedance analyzer (Agilent Technologies, Santa Clara, California) and a front end amplifier stage used to drive currents and sense voltages. Custom software was developed to drive a 1 mA current between opposing outer electrodes and sense the induced voltage between opposing central electrodes at 31 frequencies logarithmically spaced from 0.1 to 100 kHz. The ratio of induced voltage to applied current specifies the discrete electrical impedance (Z*) of the tissue sample. A multiplicative calibration factor based on the separation between the 2 PCBs is used to transform these discrete measurements to the probe independent bulk property value (z*). The inverse of bulk impedance (1/z*) defines tissue electrical admittivity (σ^*), which comprises conductivity (σ) and permittivity (ε) terms, where $\varepsilon = 2\pi f \varepsilon_0 \varepsilon_r$ with f representing applied signal frequency, ε_0 representing free space permittivity (8.85×10^{-12} F/m) and ε_r representing tissue dependent relative permittivity. σ and ε vary with applied signal frequency in tissue and are reported in mS/m. This probe senses a cylindrical volume with a fixed diameter of 3.5 mm and a height that depends on tissue sample thickness. This thickness is recorded for each specimen probed and accounted for in measurement calibration. The probe was fully characterized and validated in a previous study.12

A total of 16 admittivity spectra were recorded from each of 50 ex vivo prostates removed during radical laparoscopic prostatectomies performed by the same surgeon (JAH) at Dartmouth-Hitchcock Medical Center. In all cases measurements were begun within 30 minutes after removing the prostate from the body. Each prostate was sectioned into approximately 3 mm tissue samples at the pathology department and laid on the bench top before probing. A total of 4 locations from each of 4 prostate sections were probed

NIH-PA Author Manuscript

NIH-PA Author Manuscript

NIH-PA Author Manuscript

according to a systematic sampling approach, as previously described.12 The area probed was marked with pinholes to provide precise colocalization between recorded admittivity spectra and histological assessment (fig. 2). The study protocol received institutional review board approval and informed consent was obtained from participating subjects.

Histological Assessment

The same pathologist (AS) reviewed all regions probed and reported the proportion of individual tissue types involved at each location. To ease evaluation these proportions were limited to 10%, 25%, 33%, 50%, 66%, 75%, 90% or 100%, and tissue types included ACa, BPH, Gl, Str and other. The other grouping consisted of high grade prostatic intraepithelial neoplasia, simple and cystic atrophy, and extraprostatic adipose tissue. Primary and secondary Gleason grades were reported for all regions containing ACa.

Statistical Analysis

The tissue regions probed consisting of greater than 50% of a single tissue type were selected for analysis. In these cases each admittivity spectrum was assigned the predominant tissue type. Differences in mean admittivity properties (σ and ε) between the different tissue types were evaluated by paired testing with differences considered significant at $p < 0.05$. We also assessed ROCs associated with discriminating between ACa and all benign tissues, and between ACa and BPH, Gl and Str tissues individually. ROCs were evaluated by comparing the AUCs. This analysis was performed for σ and ε at all signal frequencies to determine the discriminatory power of the admittivity properties and the optimal signal frequencies to apply. All tests were 2-tailed. Statistical analysis was done with Stata®/IC 10 for Windows®.

Results

Of the 800 colocalized admittivity and histology pairs assessed (50 prostates × 16 spectra per prostate) 573 had a single tissue type composing more than 50% of the region probed, including ACa in 71, BPH in 165, Gl in 148, Str in 152, high grade prostatic intraepithelial neoplasia in 4, cystic atrophy in 17, simple atrophy in 14 and extraprostatic adipose tissue in 2. Other tissue types were not included in analysis because of small sample size. Table 1 lists analyzed tissue types in each prostate. In the ACa group the primary Gleason grades assigned were grade 3 in 44 and grade 4 in 27 pairs, the secondary Gleason grades were grade 3 in 40, grade 4 in 29 and grade 5 in 2, and the combined Gleason scores were 6 in 28, 7 in 28, 8 in 13 and 9 in 2. Tissue thickness in all samples was 1.1 to 6.4 mm (mean ± SD 3 ± 0.82). After calibration no significant σ or ε correlations were associated with tissue thickness at any applied signal frequencies ($p > 0.05$), confirming that the calibrated admittance properties were not influenced by the sectioning procedure.

Table 2 shows σ and ε property values for each tissue type at 0.1, 1, 10 and 100 kHz. At low frequencies (0.1 kHz) some recorded ε values were negative, which is not physically realizable. These erroneous readings resulted from extremely increased permittivity values that are not resolvable with the current instrumentation. Thus, these data were excluded from 0.1 kHz permittivity analysis, resulting in only 58 ACa, 145 BPH, 118 Gl and 85 Str ε/histology pairs being evaluated at this frequency.

Figure 3 shows mean σ and ε across the measured frequency spectrum for the different tissue types. Significant mean property differences were noted between ACa and benign tissues for several frequencies (table 3). Specifically the conductivity of ACa was significantly less than that of Str at all frequencies and significantly less than that of Gl at frequencies above 1 kHz. No significant conductivity differences were noted between ACa and BPH. The

NIH-PA Author Manuscript

NIH-PA Author Manuscript

NIH-PA Author Manuscript

permittivity of ACa was significantly larger than that of Str at all frequencies, significantly less than that of Gl at 1 and 10 kHz, and significantly less than that of BPH at 0.1 and 1 kHz. Interestingly the permittivity of ACa was significantly larger than that of all benign tissues types at 100 kHz.

The influence of Gleason score on electrical properties in the ACa group was assessed by testing the significance of the difference in mean properties when primary, secondary and combined Gleason scores were assigned as the discriminating factor. Paired tests were done between primary Gleason grades 3 and 4, secondary grades 3 and 4, and combined scores of 6 and 7, 6 and 8, and 7 and 8. The 2 secondary grade 5 and 2 combined grade 9 data sets were not included because of small sample size. Significance was assessed at 0.1, 1, 10 and 100 kHz. No significant differences were noted for conductivity at any frequency analyzed ($p > 0.05$). However, there were significant differences in some permittivity pairings. The permittivity of primary Gleason score 3 was significantly less than that of primary Gleason score 4 at 100 kHz ($p = 0.0362$). The permittivity of secondary Gleason score 3 was significantly less than that of secondary Gleason score 4 at 100 kHz ($p = 0.0152$). The permittivity of combined Gleason score 6 was significantly less than that of combined Gleason score 8 at 0.1 and 100 kHz ($p = 0.0077$ and 0.0038, respectively). The permittivity of combined Gleason score 7 was significantly less than that of a combined Gleason score 8 at 100 kHz ($p = 0.0377$).

The effectiveness of discriminating cancer from other tissue types was evaluated using ROC curves. The ACa admittivity properties of 71 pairs were compared with those of all 465 benign tissues grouped together, of BPH alone in 165, of Gl alone in 148 and of Str alone in 152. The AUC of each tissue type pairing was assessed across the full frequency spectrum for conductivity and permittivity (fig. 4). Figure 5 shows σ and ε ROC curves at the optimal frequency, defined as the frequency at the maximum AUC. The optimal frequency for discriminating ACa from all benign tissues was 15.8 kHz for σ (AUC 0.616, 95% CI 0.548–0.683) and 100 kHz for ε (AUC 0.798, 95% CI 0.735–0.861), from BPH was 0.1 kHz for σ (AUC 0.570, 95% CI 0.493–0.648) and 100 kHz for ε (AUC 0.758, 95% CI 0.684–0.832), from Gl was 25.1 kHz for σ (AUC 0.619, 95% CI 0.540–0.697) and 100 kHz for ε (AUC 0.762, 95% CI 0.688–0.836) and from Str was 0.1 kHz for σ (AUC 0.764, 95% CI 0.697–0.832) and 79.4 kHz for ε (AUC 0.878, 95% CI 0.823–0.932). Table 4 lists specificity and property thresholds at these optimal frequencies with these parameters stratified by discrete sensitivity levels.

The optimal parameter for discriminating cancer from all benign tissues grouped together was ε at 100 kHz. When high grade cancers (Gleason sum greater than 6 in 43 samples) were compared with all benign tissues, the AUC of this optimal discriminator increased to 0.823 (95% CI 0.750–0.896) and when low grade cancers (Gleason sum less than 7 in 28) were assessed, the AUC of ε at 100 kHz decreased to 0.760 (95% CI 0.650–0.869).

Discussion

It is important to establish the expected contrasts and discriminatory power provided by tissue electrical properties. This is especially critical as clinical devices are developed that gauge these properties to detect and identify ACa. Also, because these properties are frequency dependent, it is important to establish the contrasts at multiple frequencies and gauge which frequencies would provide the best potential for discriminating cancer from benign prostate. The data presented suggest that these electrical properties provide sufficient contrast for cancer detection and indicate the frequencies that might best be used as new technologies are developed.

NIH-PA Author Manuscript

NIH-PA Author Manuscript

NIH-PA Author Manuscript

The mean conductivity of all prostatic tissue types was 83 mS/m at 100 Hz and 150 mS/m at 100 kHz, and mean permittivity was 0.558 mS/m at 100 Hz and 30.3 mS/m at 100 kHz. These values are within the ranges reported for other soft tissues13 and similar to those in our previous series, in which mean conductivity was 179 mS/m and mean permittivity was 37 mS/m at 100 kHz.7 Furthermore, relationships between the different tissue types appeared to be similar and significant. Specifically the conductivity of cancer was less than that of normal tissue types (Gl and Str), which confirms our previous assertion that Str rich tissues provide an enhanced environment for current flow, ie higher conductivity.7

While the conductivity relationship between the different tissue types remained fixed across the frequency spectrum interrogated, permittivity relationships appeared to change with increasing frequency. In particular the permittivity of ACa was significantly greater than that of Str at all frequencies but less than that of BPH and Gl at frequencies less than 15.8 kHz, and larger at frequencies greater than 15.8 kHz. The variability in cellular and glandular content, size and distribution was evident between the tissue types (fig. 2), contributing to these observed permittivity differences. The inversion in how the permittivity of ACa is related to other tissue types was not observed in our previous study.7 However, the prior study included only 18 cancer lesions and we used a 2-electrode probe, which sensed larger contact impedances than the current 4-electrode probe (fig. 1). Further investigation is needed to assess the biophysical mechanism behind this spectral inversion.

The significant permittivity differences associated with different Gleason grades suggests that these electrical properties could potentially characterize how well a specific cancer region is differentiated. Cancer with Gleason grade 4 morphology has higher cellular density with less well-defined glands and pronounced glandular fusion. Grade 3 morphology has more discrete glandular profiles but they are in larger proportion and have smaller luminal spaces than benign glandular formations. The increased cell density associated with grade 4 tissues is hypothesized to provide greater permittivity because of the increased number of cell membranes, which account for the differences observed.

The discriminatory power of admittivity properties of prostatic tissues to distinguish cancer from other tissues types was evaluated by ROC analysis. When ACa was compared with all benign tissue types, the optimal frequency to distinguish tissue types using conductivity was 15.8 kHz (AUC 0.616) and using permittivity it was 100 kHz (AUC 0.798). The AUC of permittivity is higher than that reported by Thompson et al for PSA evaluation at a threshold of 3.0 ng/ml to discriminate cancer from no cancer (reported AUC 0.678).14 At a PSA threshold of 3.1 ng/ml they reported 32.2% sensitivity and 86.7% specificity. At similar 30% sensitivity conductivity provides 81.7% specificity at threshold (95 mS/m) and permittivity provides 97.0% specificity at threshold (35.4 mS/m). Sensing these electrical properties may provide a second round of screening after increased PSA is noted and may be used to eliminate the need for some biopsy procedures.

To our knowledge these results represent the most comprehensive study to date of the electrical properties of human prostate tissues and show the potential of using these properties to distinguish cancerous from benign tissues. A number of limitations in this study should be considered as clinical technologies incorporating these tissue properties are developed. The electrical properties of ex vivo tissues samples differ from those recorded in vivo. It is well established that as a tissue or organ is devascularized, the electrical properties of the tissue change. Haemmerich et al reported conductivity decreases of 53% at 10 Hz and 32% at 1 MHz in liver 2 hours after removal in an animal model.15 These changes arise from temperature changes in the tissue and the metabolic breakdown of cellular regulation. After devascularization metabolic resources are depleted, leading to cellular swelling. This swelling decreases the extracellular fluid volume available for current flow and is

NIH-PA Author Manuscript

NIH-PA Author Manuscript

NIH-PA Author Manuscript

hypothesized to be the primary cause of the observed decrease in conductivity. Similar effects are expected in radical prostatectomy specimens. To minimize this effect we collected measurements within 30 minutes of prostate removal from each patient and followed the same protocol in all. However, the interval between prostate devascularization and the time that it was provided to our team varied and depended largely on surgical conditions since the prostate was left in the body for different periods depending on the surgical plan. Regardless of when we were given the specimen, tissue temperature had achieved a thermal equilibrium of about 20C by the time that we began our probing procedure. These factors may have contributed to the modest data variability (table 2).

Another limitation is that histological analysis was semiquantitative and only tissue regions with greater than 50% of a single tissue type were selected for analysis. In cases with less than 100% of a single tissue type other secondary tissue types were present that influenced the recorded electrical properties. Analyzed tissues consisted of an average of approximately 85% of a single tissue type (table 1), suggesting that there was less than 15% of a secondary tissue type in most cases. More quantifiable methods of tissue analysis, ie using digital image processing techniques, may be used to more precisely analyze tissue morphological properties.

Also, these data were analyzed at single frequencies. Parameterizing the admittivity spectra using techniques such as those described by Halter et al12 to extract a smaller set of parameters incorporating data collected at multiple frequencies may provide enhanced discriminatory power. This approach is discussed in part II of this study.16 Sampling multiple frequencies requires longer measurement time than collecting single frequency properties but may provide improved sensitivity and specificity.

Finally, we gauged electrical properties through direct contact of the probe with tissue sections. Clinical usefulness would require gauging these properties from outside the prostate capsule and/or by introducing small, needle based sensors into the prostate.

Despite these drawbacks the evidence provided suggests that prostate tissue electrical properties might provide a new diagnostic tool for cancer detection. These properties may be sensed using electrical impedance endotomography techniques, as described by Jossinet et al,10 or using single point measurement devices.9 These data suggest that if a volume of approximately 15 mm^3 (mean probe separation of 3 mm × area of probe face 5 mm^2) can potentially be sensed with a discrete probe or an imaging device, cancerous lesions of more than 50% of this volume would potentially be identifiable.

Conclusions

Prostate tissue electrical conductivity and permittivity show promise for distinguishing cancer from benign tissues. The optimal frequencies shown by this data set are 15.8 kHz for conductivity and 100 kHz for permittivity when a tetrapolar electrode configuration is used. Sensitivity and specificity exceed those reported for current PSA screening practices at low PSA, making this an attractive addition to the clinical armamentarium for detecting ACa. Future studies of these tissue properties are suggested to gain an appreciation of how the properties differ in vivo. It is expected that magnitudes may vary with respect to the ex vivo values reported but differences between the tissue types are hypothesized to be similar.

Acknowledgments

Michael Milone digitized the micrographs.

NIH-PA Author Manuscript

NIH-PA Author Manuscript

NIH-PA Author Manuscript

Supported by United States Department of Defense Congressionally Directed Medical Research Programs Grant W81XWH-07-1-0104, the Prouty Foundation at Norris Cotton Cancer Center and United States National Institutes of Health R01 Grant CA124925.

References

1. Jemal A, Siegel R, Ward E, et al. Cancer statistics, 2008. CA Cancer J Clin. 2008; 58:71. [PubMed: 18287387]
2. Linn MM, Ball RA, Maradiegue A. Prostate-specific antigen screening: friend or foe? Urol Nurs. 2007; 27:481. [PubMed: 18217530]
3. Roberts RO, Bergstralh EJ, Peterson NR, et al. Positive and negative biopsies in the pre-prostate specific antigen and prostate specific antigen eras, 1980 to 1997. J Urol. 2000; 163:1471. [PubMed: 10751860]
4. Schwartz MJ, Hwang DH, Hung AJ, et al. Negative influence of changing biopsy practice patterns on the predictive value of prostate-specific antigen for cancer detection on prostate biopsy. Cancer. 2008; 112:1718. [PubMed: 18330908]
5. Savage L. Is an improved PSA screening test in sight? J Natl Cancer Inst. 2007; 99:1503. [PubMed: 17925529]
6. Lee BR, Roberts WW, Smith DG, et al. Bioimpedance: novel use of a minimally invasive technique for cancer localization in the intact prostate. Prostate. 1999; 39:213. [PubMed: 10334111]
7. Halter RJ, Schned AR, Heaney JA, et al. Electrical impedance spectroscopy of benign and malignant prostatic tissues. J Urol. 2008; 179:1580. [PubMed: 18295258]
8. Salomon G, Hess T, Erbersdobler A, et al. The feasibility of prostate cancer detection by triple spectroscopy. Eur Urol. 2008; 55:376. [PubMed: 18359147]
9. Kommu SS, Andrews RJ, Mah RW. Real-time multiple microsensor tissue recognition and its potential application in the management of prostate cancer. BJU Int. 2006; 97:222. [PubMed: 16430616]
10. Jossinet J, Marry E, Matias A. Electrical impedance endotomography. Phys Med Biol. 2002; 47:2189. [PubMed: 12164581]
11. Halter RJ, Hartov A, Heaney JA, et al. Electrical impedance spectroscopy of the human prostate. IEEE Trans Biomed Eng. 2007; 54:1321. [PubMed: 17605363]
12. Halter RJ, Hartov A, Paulsen KD, et al. Genetic and least squares algorithms for estimating spectral EIS parameters of prostatic tissues. Physiol Measure. 2008; 29:S111.
13. Gabriel S, Lau RW, Gabriel C. The dielectric properties of biological tissues: II. Measurements in the frequency range 10 Hz to 20 GHz. Phys Med Biol. 1996; 41:2251. [PubMed: 8938025]
14. Thompson IM, Ankerst DP, Chi C, et al. Operating characteristics of prostate-specific antigen in men with an initial PSA level of 3.0 ng/ml or lower. JAMA. 2005; 461:66. [PubMed: 15998892]
15. Haemmerich D, Ozkan OR, Tsai JZ, et al. Changes in electrical resistivity of swine liver after occlusion and postmortem. Med Biol Eng Comput. 2002; 40:29. [PubMed: 11954705]
16. Halter R, Schned A, Heaney J, et al. Electrical properties of prostatic tissues: II. Spectral admittivity properties. J Urol. 2009; 182:xxxx.

Abbreviations and Acronyms

ACa	prostate adenocarcinoma
BPH	benign prostatic hyperplasia
Gl	nonhyperplastic glandular tissue
PCB	printed circuit board
PSA	prostate specific antigen
Str	stroma

NIH-PA Author Manuscript

NIH-PA Author Manuscript

NIH-PA Author Manuscript

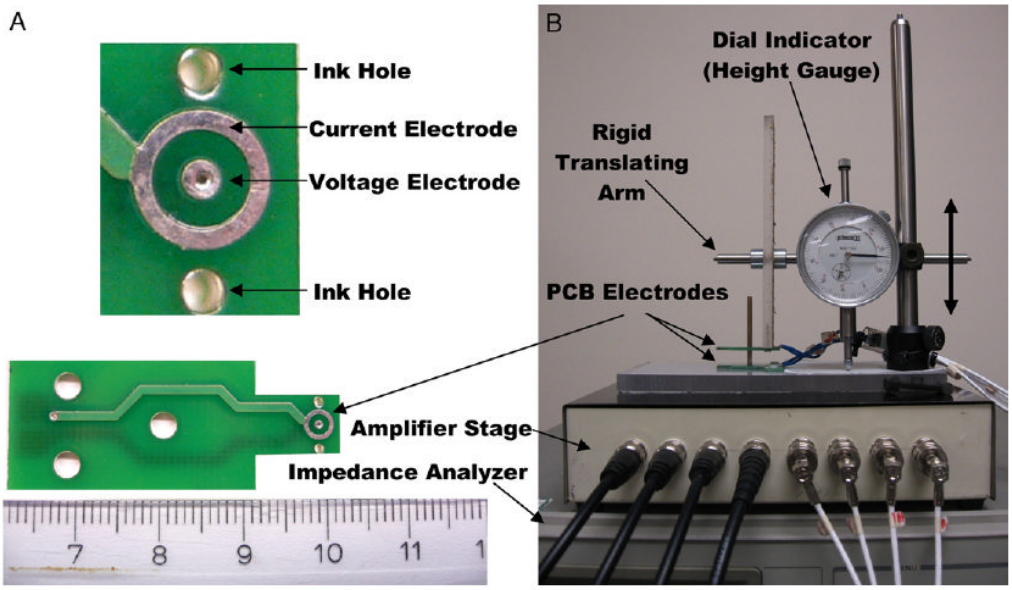

Figure 1.

Individual coaxial electrode pair PCBs (*A*, bottom) and expanded view of electrodes (*A*, top) with complete tetrapolar admittivity probe assembly (*B*). Tissue sample is placed between 2 PCB electrodes. Voltage electrode diameter is 1 mm. Current electrode has inner and outer diameter of 2.5 and 3.5 mm, respectively. Ink drop is placed in each hole with tissue in place. After removal from probe straight pins are inserted through ink dots to define location probed. Pins remain in tissue during fixation to provide visual landmarks for pathologist to locate precise region probed (fig. 2). Modified from Halter et al.12 Scale represents cm (*A*).

NIH-PA Author Manuscript

NIH-PA Author Manuscript

NIH-PA Author Manuscript

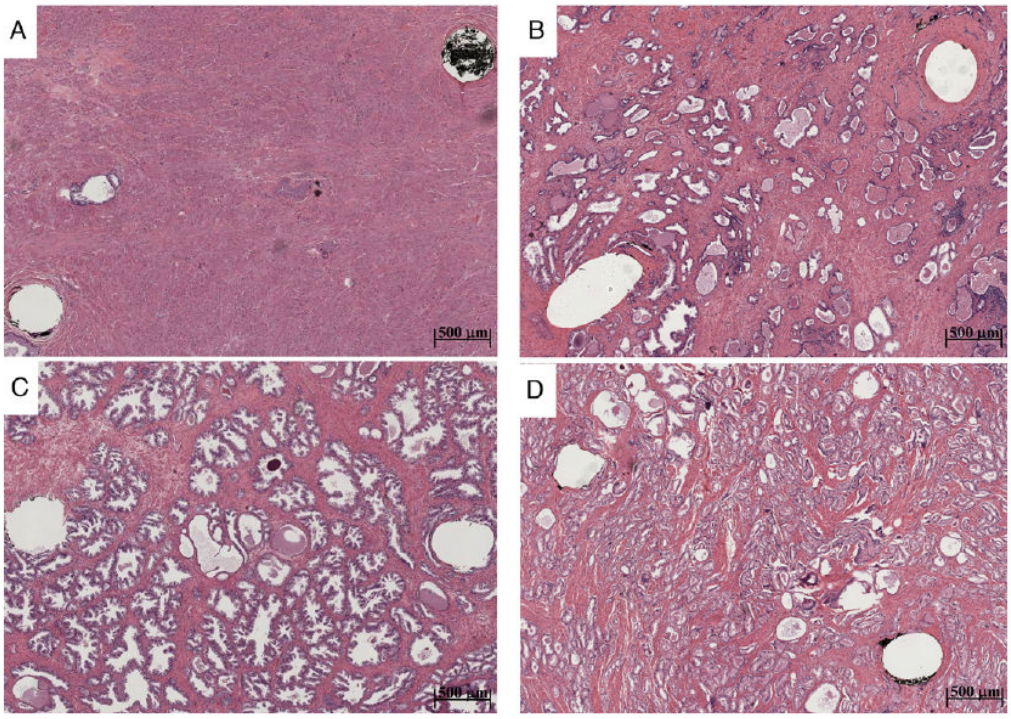

Figure 2.

Photomicrographs show 100% Str (*A*), Gl (*B*), BPH (*C*) and ACa (*D*) tissue types. Probed region corresponds to area between 2 visible pinholes remaining after tissue fixation and slide preparation. Note decreased Str content in more glandular tissue types, which we hypothesize largely influences tissue conductivity. Variability in gland size and configuration likely influences permittivity associated with different tissue types.

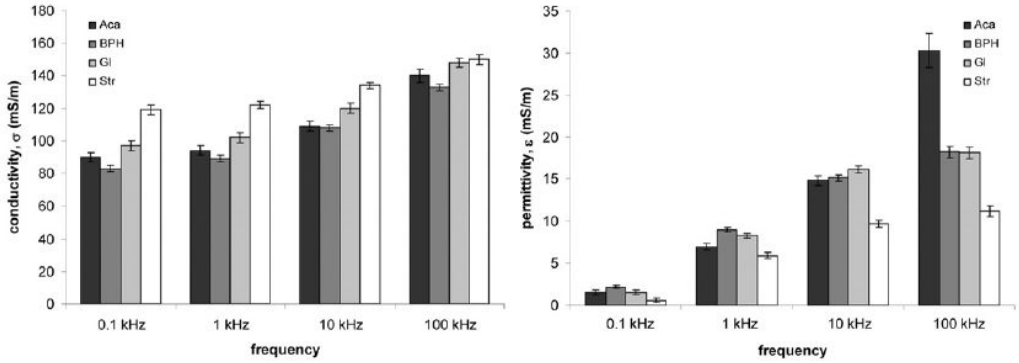

Figure 3.
Mean conductivity and permittivity at 4 acquisition frequencies, including 0.1, 1, 10 and 100 kHz. Whiskers represent SE

NIH-PA Author Manuscript
NIH-PA Author Manuscript
NIH-PA Author Manuscript

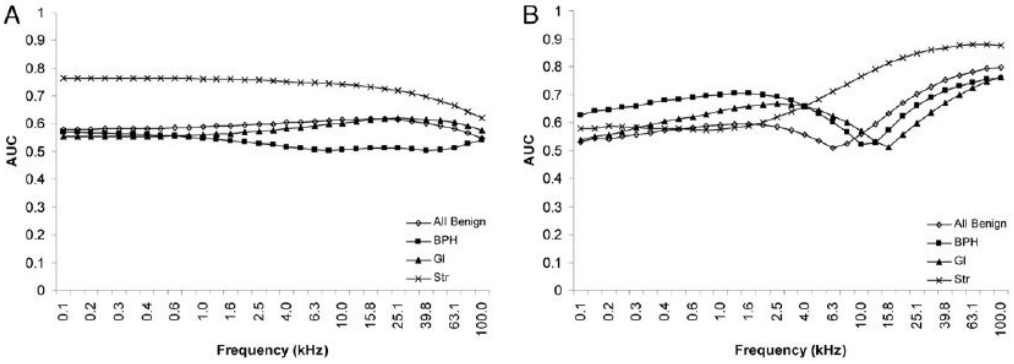

Figure 4.

AUC as function of signal frequency for conductivity (*A*) and permittivity (*B*). Note that inflection point or notch in all benign, BPH and Gl permittivity traces denotes frequency at which permittivity of cancer became greater than that of specific benign tissue (fig. 3).

NIH-PA Author Manuscript NIH-PA Author Manuscript NIH-PA Author Manuscript

NIH-PA Author Manuscript
NIH-PA Author Manuscript
NIH-PA Author Manuscript

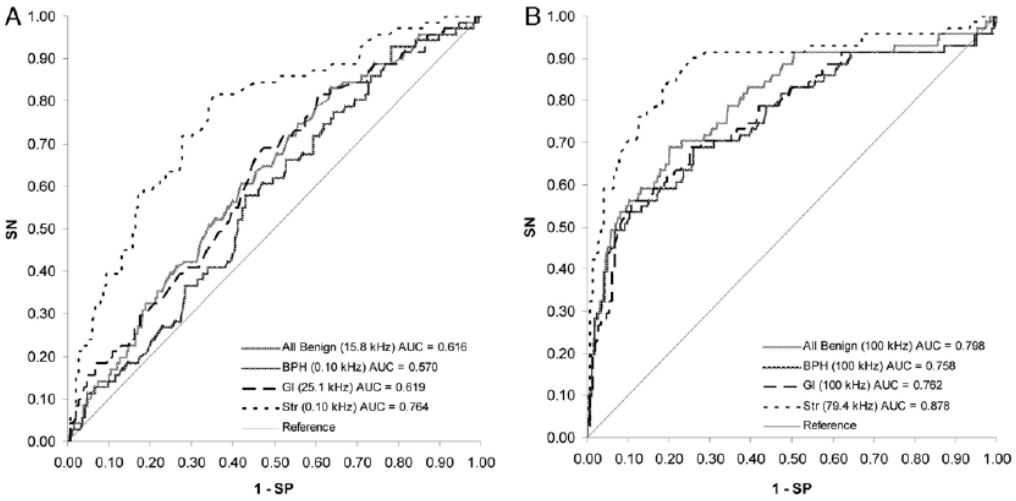

Figure 5.
ROC curves of conductivity (*A*) and permittivity (*B*) at optimal frequency. *SN*, sensitivity. *SP*, specificity

NIH-PA Author Manuscript

NIH-PA Author Manuscript

NIH-PA Author Manuscript

Table 1
Patient distribution of tissue types assessed with greater than 50% of 1 tissue type

	ACa	BPH	Gl	Str
No. cases:				
With	34	44	45	48
Without	16	6	5	2
%/Case:				
Mean	1.42	3.3	2.96	3.04
Maximum	6	10	8	7
Minimum	0	0	0	0
SD	1.5	2.85	1.97	1.58
Mean ± SD %/tissue type*	89.6 ± 12.2	87.0 ± 12.3	82.3 ± 12.9	85.7 ± 13.2

*Range 100%–66%.

NIH-PA Author Manuscript
NIH-PA Author Manuscript
NIH-PA Author Manuscript

J Urol. Author manuscript; available in PMC 2010 October 1.

Table 2

Conductivity and admittivity at 4 acquisition frequencies

	ACa (kHz)				BPH (kHz)				GI (kHz)				Str (kHz)			
	0.1	**1**	**10**	**100**	**0.1**	**1**	**10**	**100**	**0.1**	**1**	**10**	**100**	**0.1**	**1**	**10**	**100**
Conductivity:																
Minimum	38	43	53	82	35	39	54	71	29	40	51	79	6	33	64	73
25th Percentile	71	75	68	117	63	70	87	113	70	77	95	123	97	101	112	130
Median	87	92	106	135	80	87	107	134	91	100	118	146	118	122	134	149
75th Percentile	105	111	124	158	103	108	125	149	117	121	139	166	138	140	153	172
Max	166	191	219	278	167	172	186	207	224	235	261	287	211	198	220	252
Mean	90	94	109	140	83	89	108	133	97	102	120	148	119	122	134	150
SD	27	28	29	32	28	27	28	29	34	33	34	34	32	31	30	31
SE	3	3	3	4	2	2	2	2	3	3	3	3	3	2	2	3
95% CI	83–96	88–100	102–115	132–147	79–88	85–93	104–113	129–138	92–103	96–107	115–126	142–153	114–124	117–127	129–139	145–155
Permittivity:*																
Minimum	0.108	1.08	2.99	0.622	0.583	1.34	2.01	1.63	0.068	1.55	1.41	1.87	0.002	0.03	1.01	0.86
25th Percentile	0.562	4.97	12.6	28.4	1.25	6.78	11.8	13.4	0.344	6.23	12.9	13.4	.05	2.53	6.32	5.55
Median	1.58	6.89	14.9	26.7	2.36	9.24	15.3	17.1	1.80	8.03	15.6	17.3	1.22	5.77	9.92	10.3
75th Percentile	2.59	8.32	17.5	39.6	3.33	11.2	18.4	21.6	3.21	10.5	19.2	21.0	2.40	8.77	13.3	14.9
Max	17.2	17.5	29.9	91.8	10.0	18.6	30.0	77.8	11.0	17.6	30.4	63.8	9.28	24.9	28.1	49.6
Mean	1.50	6.96	14.8	30.3	2.18	9.00	15.1	18.2	1.54	8.29	16.1	18.1	0.558	5.88	9.72	11.2
SD	2.80	2.99	4.84	17.3	2.29	3.47	4.67	8.54	2.93	3.32	4.95	8.40	3.30	4.73	5.49	7.79
SE	0.333	0.355	0.574	2.05	0.178	0.270	0.364	0.665	0.241	0.273	0.407	0.690	0.268	0.383	0.445	0.632
95% CI	0.842–2.15	6.26–7.65	13.7–15.9	26.2–34.3	1.83–2.53	8.47–9.53	14.4–15.8	16.9–19.5	1.07–2.01	7.76–8.83	15.3–16.9	16.7–19.4	0.032–1.08	5.12–6.63	8.84–10.6	9.92–12.4

*Negative values recorded at 0.1 kHz are not included in statistical analysis.

NIH-PA Author Manuscript

NIH-PA Author Manuscript

NIH-PA Author Manuscript

Table 3
Significance of mean electrical property differences in ACa vs benign tissue

	Frequency p Value (paired t test equal variances)*			
	0.1 kHz	**1 kHz**	**10 kHz**	**100 kHz**
Conductivity:				
ACa vs all benign†	0.0129‡	0.0092‡	0.0015‡	0.1552
BPH§	0.0524	0.1045	0.4827	0.0752
Gl†	0.0558	0.0497‡	0.0061‡	0.04‡
Str†,‡	<0.0001	<0.0001	<0.0001	0.0076
Permittivity:				
ACa vs all benign	0.4795†	0.0578†	0.0531§	<0.0001‡,§
BPH	0.0245†,‡	<0.0001†,‡	0.3188†	<0.0001‡,§
Gl	0.4556†	0.0022†,‡	0.0411†,‡	<0.0001‡,§
Str‡,§	0.0199	0.0396	<0.0001	<0.0001

*In 536 data sets with histologically confirmed, greater than 50% individual tissue concentration.

†Mean ACa less than mean tissue type.

‡Significant ($p < 0.05$).

§Mean ACa greater than mean tissue type.

NIH-PA Author Manuscript

NIH-PA Author Manuscript

NIH-PA Author Manuscript

Table 4
Specificity and thresholds to differentiate ACa from benign tissue at stratified sensitivity

	% Sensitivity			
	90	**80**	**70**	**60**
Conductivity[*]				
Benign:				
% Specificity	19.8	37.0	46.2	57.9
Threshold (mS/m)	150	132	124	116
BPH:				
% Specificity	21.8	30.3	40.6	52.7
Threshold (mS/m)	58	67	74	83
Gl:				
% Specificity	20.3	39.9	49.3	56.8
Threshold (mS/m)	154	137	128	122
Str:				
% Specificity	29.6	65.1	72.4	79.0
Threshold (mS/m)	131	107	101	92
Permittivity[*]				
Benign				
% Specificity	49.5	62.4	77.0	83.7
Threshold (mS/m)	15.1	17.7	20.4	22.4
BPH:				
% Specificity	35.8	52.7	69.1	78.2
Threshold (mS/m)	15.1	17.7	20.4	22.4
Gl:				
% Specificity	37.8	52.7	72.3	81.1
Threshold (mS/m)	15.1	17.5	20.2	22.1
Str:				
% Specificity	75	81.6	90.1	93.4
Threshold (mS/m)	15.4	17.5	20.2	22.1

[*]Values are associated with properties evaluated at optimal frequency.